Available online at www.sciencedirect.com

ScienceDirect

Geochimica et Cosmochimica Acta 305 (2021) 306–322

Geochimica et Cosmochimica Acta

www.elsevier.com/locate/gca

Planktic foraminiferal Na/Ca: A potential proxy for seawater calcium concentration

Xiaoli Zhou [a,*], Yair Rosenthal [a,b], Laura Haynes [c], Weimin Si [d], David Evans [e], Kuo-Fang Huang [f], Bärbel Hönisch [g], Jonathan Erez [h]

[a] Department of Marine and Coastal Science, Rutgers University, New Brunswick, NJ 08854, USA
[b] Department of Earth and Planetary Sciences, Rutgers University, New Brunswick, NJ 08854, USA
[c] Department of Earth Science and Geography, Vassar College, Poughkeepsie, NY 12604, USA
[d] Department of Earth, Environmental, and Planetary Sciences, Brown University, Providence, RI 02912, USA
[e] Institute of Geosciences, Goethe University Frankfurt, 60438 Frankfurt am Main, Germany
[f] Institute of Earth Sciences, Academia Sinica, Nangang, Taipei 11529, Taiwan
[g] Lamont-Doherty Earth Observatory and Department of Earth and Environmental Sciences of Columbia University, Palisades, NY 10964, USA
[h] Institute of Earth Sciences, The Hebrew University of Jerusalem, Israel

Received 3 November 2020; accepted in revised form 3 April 2021; available online 21 April 2021

Abstract

The reconstruction of seawater calcium concentration ($[Ca^{2+}]_{SW}$) in the geologic past is crucial to our understanding of biogeochemical processes and elemental cycling as linked to long-term climate change. Published $[Ca^{2+}]_{SW}$ estimates for the Cenozoic differ from each other in both the direction and magnitude of the change, and are associated with large uncertainties. Here we demonstrate the potential of Na/Ca in planktic foraminifera as a new proxy for reconstructing Cenozoic variations in seawater Na/Ca. Because of the long oceanic residence time of Na^+ ($\gg$50 Myr), variations in foraminiferal Na/Ca should in principle reflect changes in $[Ca^{2+}]_{SW}$. Our culture experiments on live planktic species validate the approach, showing that foraminiferal Na/Ca responds to changes in $[Ca^{2+}]_{SW}$ when $[Na^+]_{SW}$ is kept constant, consistent with previous experiments on a shallow water benthic foraminifer and on inorganic calcite. The culture study suggests that planktic Na/Ca is affected, to a small extent, by calcite saturation state ($\Omega_{calcite}$) but not resolvably affected by temperature or salinity. A core tops transect of the planktic foraminifer *Trilobatus sacculifer* shows similar decreasing trends in Na/Ca and Sr/Ca with water depth that can be associated with dissolution of the tests. The strong covariance with Sr supports the hypothesis that a dominant fraction of the Na resides in lattice positions within the calcite test.

Down core planktic foraminiferal records from the Atlantic and Pacific Oceans consistently show 13–28% lower Na/Ca during the mid-Miocene than during the late Pleistocene. After considering the effects of temperature, salinity and diagenesis, we conclude that the observed down core decrease in Na/Ca primarily reflects changes in seawater calcium concentration. Using the calibrations generated from our culture experiments and core top data we reconstructed $[Ca^{2+}]_{SW}$, suggesting $[Ca^{2+}]_{SW}$ in the mid-Miocene was 46 ± 22% higher than at present, and decreased toward present with a pattern resembling the Neogene climate evolution represented by the benthic $\delta^{18}O$ record. The new reconstruction of $[Ca^{2+}]_{SW}$ for the past 16 Myr narrows the range suggested by other $[Ca^{2+}]_{SW}$ proxies, and potentially offers a new way to generate continuous records of seawater calcium concentration at sub-million years resolution.

Keywords: Paleoproxy; Planktic foraminiferal Na/Ca; Seawater Ca concentration; Neogene

* Corresponding author at: School of Ocean and Earth Science, Tongji University, Shanghai 200092, China.
E-mail address: xlzhou@tongji.edu.cn (X. Zhou).

https://doi.org/10.1016/j.gca.2021.04.012
0016-7037/

1. INTRODUCTION

Reconstructions of seawater calcium concentration ($[Ca^{2+}]_{SW}$) are key to better understanding long-term climate change because of their links to chemical weathering of silicate rocks on land and the precipitation and dissolution of carbonate minerals in the ocean, two processes that regulate long-term changes in atmospheric CO_2 (Berner and Kothavala, 2001). Because Ca has the shortest oceanic residence time (~1 Myr) of the major ions in seawater, variations in $[Ca^{2+}]_{SW}$ could have evolved with late Neogene climate and the global carbon system, including ocean alkalinity and atmospheric CO_2 (Urey, 1952). Discrete estimates from fluid inclusions in halites formed from brine solutions have provided the most widely cited reconstructions of $[Ca^{2+}]_{SW}$ (e.g., Horita et al., 2002; Lowenstein et al., 2003; Brennan et al., 2013) (Fig. 1). This method is, however, limited by the low temporal sample coverage of evaporite sequences (e.g., only a few in the Neogene) and the fact that the calcium concentration was estimated indirectly from K^+ and SO_4^{2-} concentrations, because most Ca is removed in the form of $CaCO_3$ and $CaSO_4$ from Cenozoic halite-hosted fluid inclusions (Horita et al., 2002; Brennan et al., 2013). Subsequent reconstructions of $[Ca^{2+}]_{SW}$ are based on modeling of Ca-isotope records in nannofossil ooze, planktic foraminifera, and marine barite (Heuser et al., 2005; Griffith et al., 2008a; Fantle, 2010). Within errors, these reconstructions either showed a local high at ~ 10–11 Ma or decreased gradually with cyclic changes over the late Neogene, with individual proxies differing from each other by as much as 10 mmol/kg in the mid- to late-Miocene (Fig. 1). The difference between these records may reflect multiple controls on the calcium isotopic composition of seawater, such as temporal variations in the magnitude and the Ca isotope of continental weathering, dolomitization, isotope fractionation between seawater and carbonate, decoupled Ca and carbonate influxes to the ocean, and shifts in depositional mode of $CaCO_3$ in the ocean (Heuser et al., 2005; Griffith et al., 2008a; Fantle, 2010). Thus, a more direct proxy of seawater calcium concentration with a higher temporal resolution is needed. This will allow more accurate corrections on other proxy records that is affected by $[Ca^{2+}]_{SW}$. For instance, high-resolution $[Ca^{2+}]_{SW}$ record, combined with $[Mg^{2+}]_{SW}$ record, can be used to estimate the effect of seawater Mg/Ca on the Mg/Ca thermometer. Reconstructing the concentrations of calcium and other major ions also provides an important constraint allowing, together with other data, progression towards a robust reconstruction of the atmospheric CO_2 concentration (and therefore Earth's climate) over geological time.

In contrast to Ca, sodium (Na^+) has a much longer oceanic residence time (τNa is ~ 50–100 Myr; Broecker and Peng, 1982; Sarmiento and Gruber, 2006), such that its concentration has likely not changed significantly throughout the Cenozoic. Based on fluid inclusion data and charge balance, Zeebe and Tyrrell (2019) suggests that $[Na^+]_{SW}$ was constant within 2% during the past ~ 60 million years. A novel opportunity for reconstructing $[Ca^{2+}]_{SW}$ comes from a recent culturing study, which demonstrates that the Na/Ca ratio in the shallow water benthic foraminifer *Operculina ammonoides* changes when solution $[Ca^{2+}]$ varies at constant $[Na^+]$ (Hauzer et al., 2018). Thus, on million-year time scales, variations in foraminiferal Na/Ca should, in principle, reflect changes in $[Ca^{2+}]_{SW}$, potentially offering an independent approach for studying the oceanic

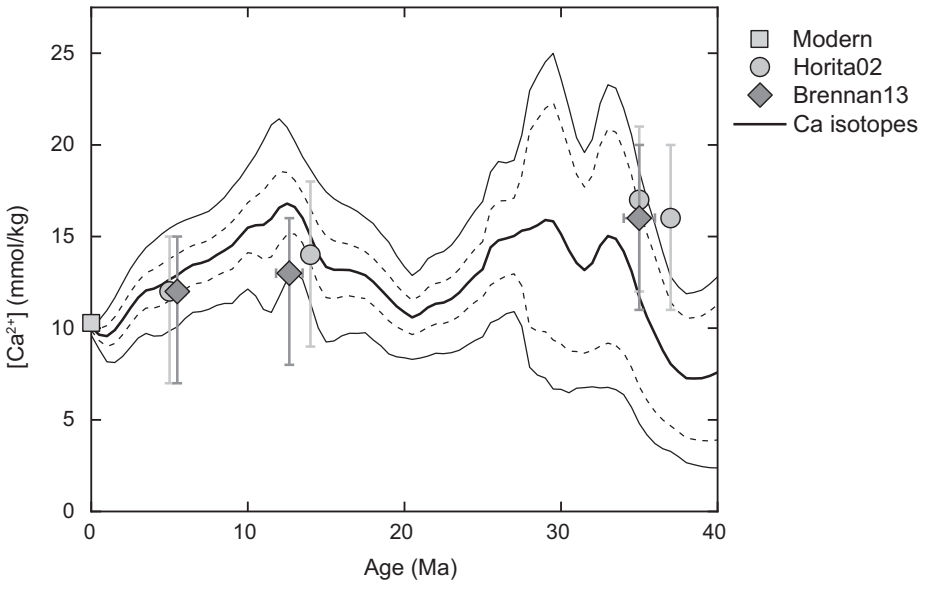

Fig. 1. **Existing Ca proxies based on fluid inclusions and Ca isotopes** (Horita et al., 2002; Heuser et al., 2005; Griffith et al., 2008b; Fantle, 2010; Brennan et al., 2013). The thick line represents the average value of the three Ca isotope records. The dashed and thin solid lines represent the standard error of the mean and the standard deviation of the mean values, respectively. The light grey circles and dark grey diamonds denote discrete fluid inclusion records with errors, and the square denotes modern ocean value. (For interpretation of the references to colour in this figure legend, the reader is referred to the web version of this article.)

Ca budget from the same samples as used for reconstructing other seawater properties (e.g., temperature and pH).

Here we combine culture experiments of three species of planktic foraminifera grown under variable solution [Ca^{2+}] with core top and down core studies to test the potential of using planktic foraminiferal Na/Ca as a proxy for seawater Ca^{2+} concentration. We use the culture results to demonstrate the response of planktic Na/Ca to changes in solution [Ca^{2+}], and investigate the possible influence of other environmental variables on Na/Ca (e.g., temperature, salinity, and carbonate saturation state). Core top and down core Na/Ca records from *Trilobatus sacculifer*, a planktic species that evolved in the mid-Miocene, are used to assess the proxy's potential for reconstructing seawater [Ca^{2+}] over the last 16 Myr. To better understand the controls on the incorporation and preservation of Na/Ca in the planktic tests and its reliability as a proxy for seawater [Ca^{2+}], we compare our Na/Ca data with Sr/Ca ratios measured on the same samples, which allows us to evaluate the importance of diagenetic vs. primary effects.

2. MATERIALS AND METHODS

2.1. Culture experiments with planktic foraminifera

The first order response of foraminiferal Na/Ca to changes in $[Ca^{2+}]_{SW}$ was investigated via culture experiments with three planktic foraminifera species – *Globigerinoides ruber* (pink), *T. sacculifer*, and *Orbulina universa*. The culture experiments were initially designed to investigate the response of trace element content in foraminifera to changes in solution chemistry, including major ions [Mg^{2+}] and [Ca^{2+}], total boron concentration ($[B]_T$) and carbonate chemistry such as DIC and pH. The experiment results on foraminiferal B/Ca were published in Haynes et al. (2017, 2019) and the culturing procedures and experimental setup were discussed in detail in these papers. Here we only discuss procedures that are relevant to solution [Ca^{2+}] and foraminiferal Na/Ca.

Culture experiments with variable solution [Ca^{2+}] were carried out at the Wrigley Institute for Environmental Studies on Santa Catalina Island in the summer of 2013 and at the Isla Magueyes Marine Science Laboratory in Puerto Rico in the spring of 2010 and 2015. For all three species, solution [Ca^{2+}] was increased from ~ 10 (modern seawater concentration) to 20 mmol/kg by adding $CaCl_2 \cdot 6H_2O$ to natural filtered seawater, while keeping all other ion concentrations the same as modern seawater. For *O. universa*, an additional experiment was conducted at 15 mmol/kg [Ca^{2+}]. We also discuss here the results from experiments where [Ca^{2+}] was varied in tandem with [Mg^{2+}], pH, and DIC concentrations in all three species. In these experiments, solutions were prepared by mixing natural and artificial seawater at a 1:1 ratio to reach target values of 20 mmol/kg [Ca^{2+}] and 30 mmol/kg [Mg^{2+}]. Salinity in these experiments was held constant at 33.1–33.4 in experiments on Santa Catalina Island and at 35.7–36.0 in Puerto Rico experiments. The addition of $CaCl_2$ salts in the high [Ca^{2+}] experiments caused a slight increase in salinity of < 1.

The solution DIC was varied via addition of $NaHCO_3$ to reach target values of 1500–3000 μmol/kg for *G. ruber* and *T. sacculifer* and 1000–4000 μmol/kg for *O. universa*. Target pH values were altered via subsequent addition with NaOH or HCl. For DIC experiments, pH was held constant at ~ 7.9; for pH experiments, pH ranged from 7.5-8.2 on the total scale. Consequently, alkalinity varied in both our pH and DIC experiments. The small variation in solution [Na^+] imposed by addition of NaOH was insignificant relative to the large amount of Na^+ in the sea water medium.

Elemental compositions of seawater solutions were determined via simultaneous ICP-Optical Emission Spectrometer at the Australian National University (Varian Vista Pro Axial). Initial and final seawater Na/Ca values were averaged to determine experimental values for Puerto Rico experiments. The relative standard deviation on all seawater [Na^+] measurements across the experiments was only 1.3%. [Na^+] data were not measured from Santa Catalina Island experiments, but [Ca^{2+}] was measured. Solution Na/Ca for these experiments is estimated based on Na/Ca measurements made on Puerto Rico seawaters, assuming a constant Na/Ca ratio of seawater and correcting for differences in salinity. Because [Ca^{2+}] and [Mg^{2+}] were the only variable ion concentrations in these experiments, and Na^+ and Ca^{2+} both behave conservatively in natural seawater (Broecker and Peng, 1982), we are confident in these estimates. Details of the solution Na/Ca and foraminiferal Na/Ca measurements are given in the Supplementary Table (Table S2). We also compiled some important data about the culture solution chemistry other than solution Na/Ca from the published literature (Haynes et al., 2017, 2019).

Before being placed into their respective experimental seawater jars, the initial size of each individual foraminifer was measured. After the foraminifera completed gametogenesis, tests were rinsed with Milli-Q water, their largest diameter was measured, and tests were archived for later analysis. The juvenile trochospiral of *O. universa* shells is negligible relative to the much larger and heavier adult spherical chamber and entire shells were therefore analyzed for this species. In contrast, the chambers of *G. ruber* and *T. sacculifer* secreted in laboratory culture were amputated from the juvenile chambers grown in the ocean prior to collection, and their sizes were determined by comparing final and collection shell diameters.

Species-specific chambers from each experiment were pooled and cleaned according to the methods of Russell et al. (2004) and Allen et al. (2012). Briefly, samples were oxidized twice with a solution composed of equal parts 0.1 N NaOH and 30% H_2O_2 at 70-80 ℃ to remove organic matter. Samples were rinsed 3x with MilliQ-H_2O, transferred to acid-cleaned vials, weak acid leached for 30 s, and rinsed 3x more with MilliQ-H_2O. Reductive cleaning was omitted because unlike sedimentary material, the only contaminant on these samples is remnant organic matter. Samples were then dissolved in 100 μL 0.065 N HNO_3, diluted to 350–400 μL with 0.5 N HNO_3 and analyzed for trace element ratios as described in Section 2.4.

2.2. Core top and down core studies

Na/Ca and Sr/Ca ratios were measured in *T. sacculifer* in 35 core top samples (300–355 μm size) from depth transects on the Ontong Java Plateau (OJP) and in the South China Sea (SCS), and in 164 down core samples from the Pacific (ODP 806, 807, 804, 1237, and IODP U1337), Atlantic (DSDP 608, ODP 667, 925, 926 and 1264,) and Indian (ODP 758) Ocean (Fig. S1). The core top samples span water depths of 1618–3710 meters from the OJP and of 329–2841 meters from the SCS; all samples are from the top 11 cm of the sediments. The down core samples span water depths of 2505–4463 meters in the modern ocean, and cover a temporal range of 0–16 Ma. Age models for all sites are from Si and Rosenthal (2019) except for Sites U1337 and 926, which are based on the biostratigraphic, paleomagnetic, and benthic foraminiferal isotope records (Shipboard Scientific Party, 1995; Expedition 320/321 Scientists, 2010; Wilkens et al., 2017).

Hydrographic data for OJP and all the down core samples were derived from world ocean databases GLODAP v1.1 and v2 (Key et al., 2004; Olsen et al., 2016). Considering the low resolution of available hydrographic data in GLODAP dataset near each site, we compiled hydrographic data ± 1–5 degrees of latitude and longitude nearby each site from GLODAP v2, and anthropogenic CO_2 data from nearby sites from GLODAP v1.1, which was subtracted from DIC in an attempt to account for anthropogenic influences. Hydrographic data for SCS samples are from the SEATS time-series in the northern SCS (Chou et al., 2007). The carbonate saturation ($\Omega_{calcite}$) was calculated by CO2SYS_v2.3.xls (Pelletier et al., 2007) using dissociation constants of carbonic acid from Hansson and Mehrbach refit by Dickson and Millero (1987), that of HSO_4^-, HF, and total [B] from Dickson (1990), Perez and Fraga (1987), and Lee et al. (2010), respectively. Thereafter, LOWESS analysis with a smoothing factor between 0.1–0.2 was performed in MATLAB to generate water column profiles for $\Omega_{calcite}$, which were subsequently used to estimate *in situ* values for our samples by linear interpolation (Table S1).

2.3. Cleaning methods

The core top and down core sediments were disaggregated over the course of ~ 8 hours by shaking in deionized water, and then washed through a 63 μm mesh to remove silt and clay. *Trilobatus sacculifer* specimens were handpicked under a microscope from the > 250 μm fraction; when available, relatively large specimens were preferentially picked. Samples from the South China Sea were picked from the 300–355 μm fraction. Each sample was composed of 10–20 individual tests, which were weighed except for samples from the Ontong Java Plateau, from which a separate set of specimens from the 300–355 μm fraction were handpicked and weighed. After weighing, samples were crushed and cleaned for trace metal analysis following the full reductive-oxidative protocol of Boyle and Keigwin (1985) modified by Rosenthal et al. (1997). Organic matter was oxidized following these methods using a 30 mL mixed solution containing 100 μL of 30% H_2O_2 and an alkaline buffer. In some of the samples that were previously analyzed specifically for Mg/Ca studies, the oxidizing solution was buffered with 0.1 N NaOH, followed by 3x Milli-Q water rinses to eliminate any trace of NaOH. Later, once we started to develop the Na/Ca proxy, we replaced NaOH with 5% NH_4OH for oxidizing solution, intended to reduce the risk of potential contamination from NaOH. This new cleaning method is also followed by 3x Milli-Q water rinses.

To verify that samples treated with the NaOH buffer were not contaminated, we compared Na/Ca ratios of several species of planktic foraminifera from a box core collected on the Ontong Java Plateau. The samples were either cleaned with the traditional 0.1 M NaOH-buffer method or with the 5% NH_4OH buffer. Our test shows the Na/Ca ratios obtained by the two methods are consistent within ~ 5% without any systematic offset (Fig. S2), suggesting that the Milli-Q water rinses efficiently removed the buffer. For each cleaning method, the reproducibility obtained from measurements on splits of the same sample is typically better than 2%. Thus, we conclude that data generated by the two methods applied here are not affected by the cleaning process. The comparison of other trace element data such as Mg/Ca and B/Ca suggests that the NH_4OH buffer is as effective as the NaOH buffer in terms of removing organic matter. Therefore, for future work on Na/Ca we recommend the use of NH_4OH as a buffer solution.

2.4. Analytical methods

Following cleaning, samples were dissolved in 100 μL 0.065 N HNO_3 and centrifuged for 10 minutes at 10,000 rpm to concentrate any undissolved solids to the bottom of the vials. Roughly 95 μL of the supernatant was diluted to 350–400 μL with 0.5 N HNO_3 and analyzed for trace elements using an Element-XR sector-field ICP-MS following the method developed by Rosenthal et al. (1999). Repeat analyses of standard solutions with the same elemental ratios (El/Ca) but different Ca^{2+} concentrations ($[Ca^{2+}] = 1.5$ mM to 8 mM) were used to quantify and correct for matrix effects. Repeat analyses of standard solutions with different Na/Ca ratios (Na/Ca = 6 to 16 mmol/mol) were used to assess long-term reproducibility. The long-term accuracy is less than 4% for Na/Ca ranging between 6 and 16 mmol/mol and the precision is ~ 1% RSD for Na/Ca = 1.45 mmol/mol.

3. RESULTS

3.1. Culture experiments with planktic foraminifera

Elemental analysis of chambers secreted under experimental conditions shows a decrease in the $(Na/Ca)_{test}$ of all three species with increasing $[Ca^{2+}]_{SW}$ (decreasing $(Na/Ca)_{SW}$) in the culturing media (Tables S2 and S5, Fig. 2A). We observe that the $(Na/Ca)_{test}$ in the tests of *G. ruber* is significantly higher than in *T. sacculifer* and *O. universa*, which show similar ratios. However, all three species exhibit a similar sensitivity (i.e., slope) of Na/Ca

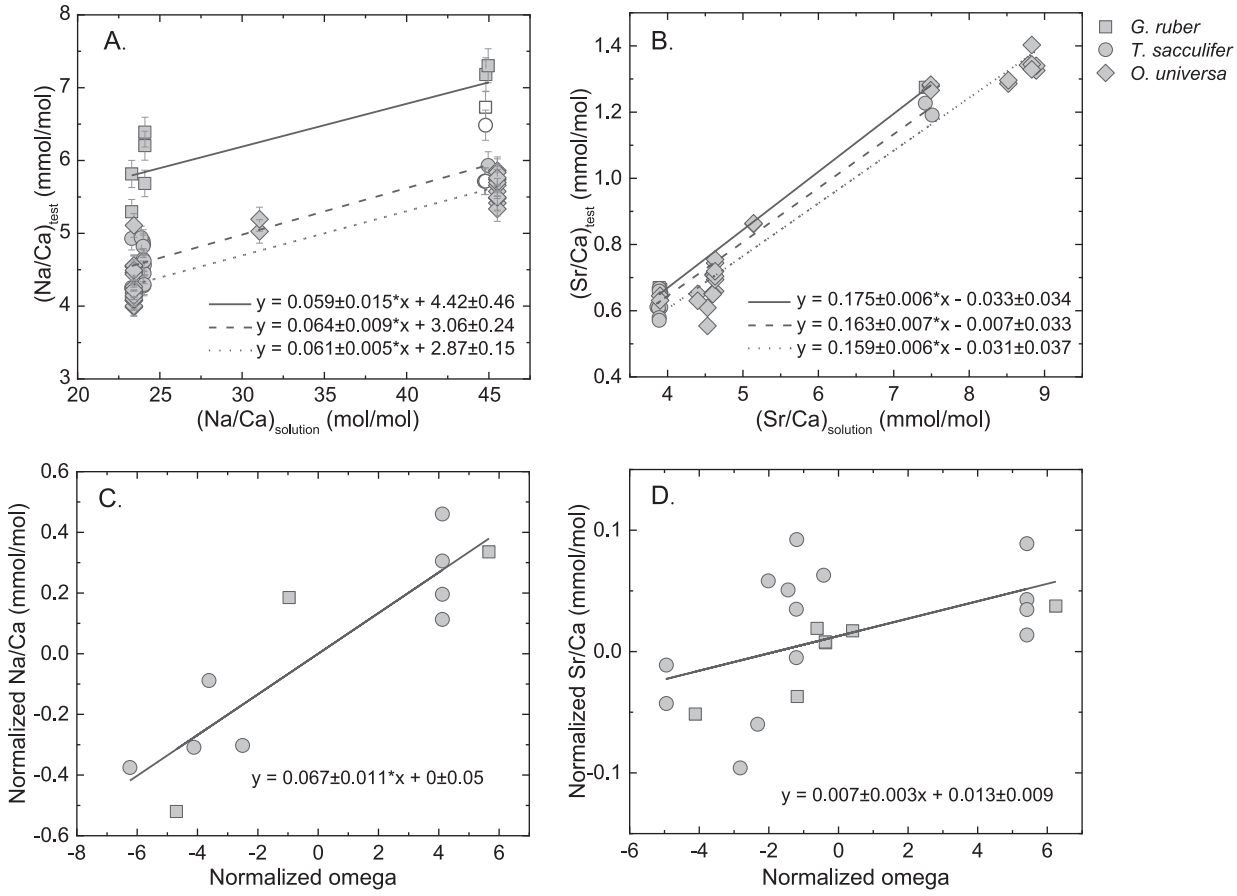

Fig. 2. **Planktic Na/Ca and Sr/Ca records from the culture experiments.** In A and B, Na/Ca and Sr/Ca in *G. ruber* (squares, this study and data from the ambient experiment in Allen et al. (2016)), *T. sacculifer* (circles, this study and data from the ambient experiments in Allen et al. (2016)), and *O. universa* (diamonds, this study) are plotted with Na/Ca and Sr/Ca of the culture solutions, respectively. Open symbols represent data from Allen et al. (2016). Linear regression for each species suggest positive correlations between Na/Ca and Sr/Ca in foraminifera versus in the solution. In C and D, foraminiferal Na/Ca and Sr/Ca in *G. ruber* and *T. sacculifer* from Allen et al. (2016) are normalized to their average values and plotted with $\Omega_{calcite}$ that is also normalized to its average value for each species. Data from the two species are combined to yield linear regression for Na/Ca and Sr/Ca versus the normalized $\Omega_{calcite}$, respectively, suggesting a positive correlation between Na/Ca and $\Omega_{calcite}$ but an insignificant correlation between Sr/Ca and $\Omega_{calcite}$. For details in statistical analysis, please refer to Table S5. (For interpretation of the references to colour in this figure legend, the reader is referred to the web version of this article.)

versus $[Ca^{2+}]$ in the culture solutions, though with different non-zero intercepts. Sr/Ca in the three planktic species also shows a decreasing trend with increasing $[Ca^{2+}]_{SW}$ (i.e., decreasing $(Sr/Ca)_{SW}$; Table S5). Unlike Na/Ca, Sr/Ca exhibits nonsignificant interspecies differences and all the specific regressions nearly go through the origin (Fig. 2B).

Carbonate system variables were also modified in the high $[Ca^{2+}]$/low $[Mg^{2+}]$ ($[Ca^{2+}] = 18.4 \pm 0.3$ mmol/kg, $(Mg/Ca)_{SW} = 1.5$ mol/mol) experiments. To isolate the influence of changes in the carbonate system, we use data from Allen et al. (2016) to estimate the sensitivity of $(Na/Ca)_{test}$ and $(Sr/Ca)_{test}$ to changes in calcite saturation of the growing medium ($\Omega_{calcite}$) under modern $[Ca^{2+}]_{SW}$ (Table S5, Fig. 2C-D).

3.2. Core top and down core records of planktic foraminifera

Core tops Na/Ca and Sr/Ca in *T. sacculifer* both decrease with increasing water depth, but to a different degree (Table S3). Na/Ca decreases at a rate of 0.40 mmol/mol per kilometer from 329 to 2841 meters in the South China Sea and 0.26 mmol/mol per kilometer from 1618 to 3710 meters on the Ontong Java Plateau (Fig. 3). In the same samples as for Na/Ca, Sr/Ca decreases at a rate of 0.033 and 0.024 mmol/mol per kilometer in the South China Sea and on the Ontong Java Plateau, respectively. The average test weight of the analyzed *T. sacculifer* specimens decreases with water depth at a rate of 3.5 μg/km in both transects.

The down core Na/Ca and Sr/Ca records from multiple sites display coherent long-term trends, increasing from 16 to 12–14 Ma, reaching a local high, then decreasing to ~ 8 Ma, and monotonically increasing toward the present (Fig. 4A-B; Table S4). For Na/Ca, the records from the Atlantic Ocean are slightly higher than those from the Pacific Ocean, whereas an inter-basin difference is less prominent for Sr/Ca, especially between 7 Ma and present (Fig. 4A-B).

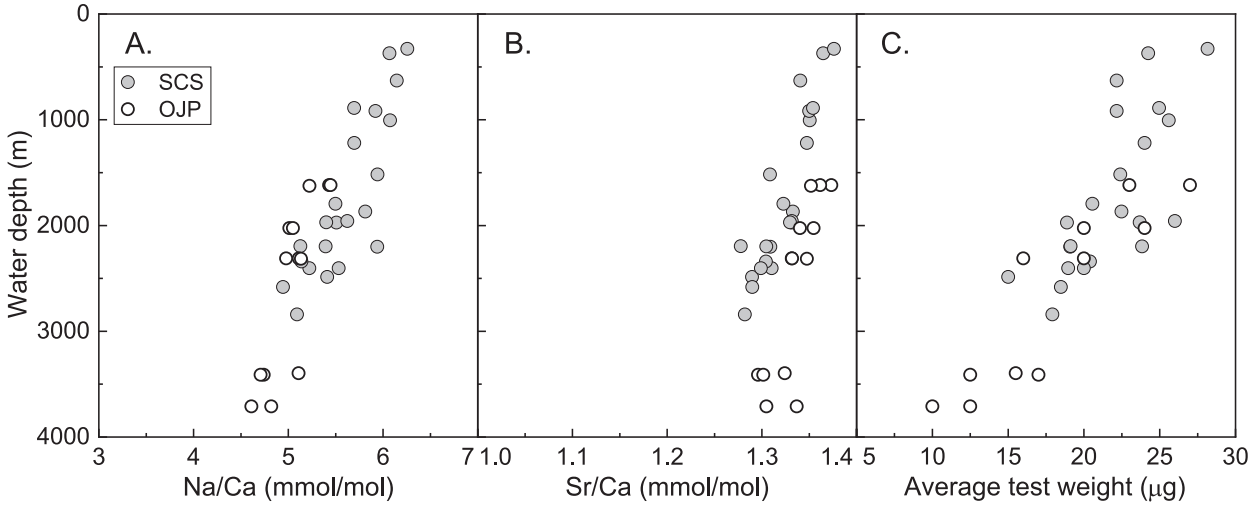

Fig. 3. **Na/Ca and Sr/Ca records and the average test weight of core top *T. sacculifer*.** Water depth profiles are plotted for Na/Ca (A), Sr/Ca (B) and the average test weight (C) of *T. sacculifer* from core top sediments from the Ontong Java Plateau (open circles) and the South China Sea (filled circles). The decrease of test weight with water depth (C) indicates a dissolution trend that is significant below 2000 m. Similarly, with increased water depth and weight loss the Na/Ca (A) and Sr/Ca (B) decrease significantly (see main text). (For interpretation of the references to colour in this figure legend, the reader is referred to the web version of this article.)

4. DISCUSSION

In order to interpret our foraminiferal Na/Ca records in terms of changes in seawater [Ca^{2+}], we first discuss the incorporation of Na into foraminiferal test, then use the culture data to calibrate the sensitivity of foraminiferal Na/Ca to changes in seawater [Ca^{2+}] (i.e., the slope of that relationship). We then assess the possibility that diagenetic processes, such as dissolution and recrystallization, might have compromised the reliability of foraminiferal Na/Ca as a proxy for past seawater [Ca^{2+}]. Combining all the information, we evaluate the down core data obtained from *T. sacculifer*. We also compare Na/Ca with Sr/Ca data to better constrain the geochemical controls on planktic foraminiferal Na/Ca.

4.1. Incorporation of Na into calcite

Early inorganic precipitation experiments focused on the co-precipitation of Na in $CaCO_3$ as a potential proxy for paleo-salinity. Among those were Ishikawa and Ichikuni (1984), who concluded that Na^+ inhabits interstitial lattice positions in the inorganic calcite based on their argument that Na/Ca ratios in precipitated calcite were independent of calcium concentration. However, pH was also varied in their experiments, which may have compromised the response of Na/Ca in synthetic calcite to the changes in solution [Ca^{2+}] (Ishikawa and Ichikuni, 1984). White (1978) and Okumura and Kitano (1986) observed an increase in Na^+ content in synthetic calcite with increasing Mg^{2+} content, arguing that the substitution of Mg^{2+} for Ca^{2+} creates significant distortion favoring the incorporation of Na^+ (Busenberg and Plummer, 1985). The influence of Mg^{2+} on Na^+ incorporation is substantiated by culture studies that also display a strong co-variation between the distribution coefficients of Na/Ca and Mg/Ca in high-Mg calcite foraminiferal tests of *Operculina ammonoides* (Evans et al., 2015; Hauzer et al., 2018). A possible mechanism for this observation is proposed by the mineralogical studies of Yoshimura et al. (2017) who suggested substitution of Na^+ for Ca^{2+} sites in the lattice structures, involving charge compensation through the creation of CO_3^{2-} vacancies. The strong covariance between Na and Sr observed in our core top and down core data (Figs. 3 and 4) supports this hypothesis suggesting that, similar to Sr^{2+}, a large portion of the Na^+ content in fossil tests of *T. sacculifer* is also in the calcite lattice. We note that the relative changes in Na/Ca and Sr/Ca in response to the changes in [Ca^{2+}] of the solutions are similar in all three species (Fig. 2A-B). A likely explanation is that like Sr^{2+}, the changes in Na^+ are also due to substitution with Ca^{2+} in the lattice. However, differences in the absolute Na/Ca values among the species and the enriched Na/Ca relative to Sr/Ca in the high $[Ca^{2+}]_{sw}$ culture experiments raise the possibility of an additional, Na-enriched phase in pristine foraminifera, such as those collected in laboratory culture (Figs. 2A and S4).

Minor amounts of Na^+ may also occur in organic matter or in seawater inclusions in foraminiferal tests (Yoshimura et al., 2017). In fact, Na-, and Mg-rich bands have been observed in the tests of several cultured planktic foraminifera species, where they are associated with organic layers such as the primary organic sheet (POS) and alternate with low-Na bands (Branson et al., 2016; Bonnin et al., 2019). Na/Ca profiles of foraminiferal test walls of cultured *O. universa* show that Na/Ca in the POS is ~ 25–30% higher than background values (Branson et al., 2016; Bonnin et al., 2019). The thickness of the POS is estimated to be less than 1 μm (Branson et al., 2016), and the thickness of foraminiferal test walls roughly ranges between 10–30 μm according to the image scales of foraminiferal test walls (Bonnin et al. 2019). As a result, the high Na/Ca values at the POS in this species can only raise the bulk Na/Ca

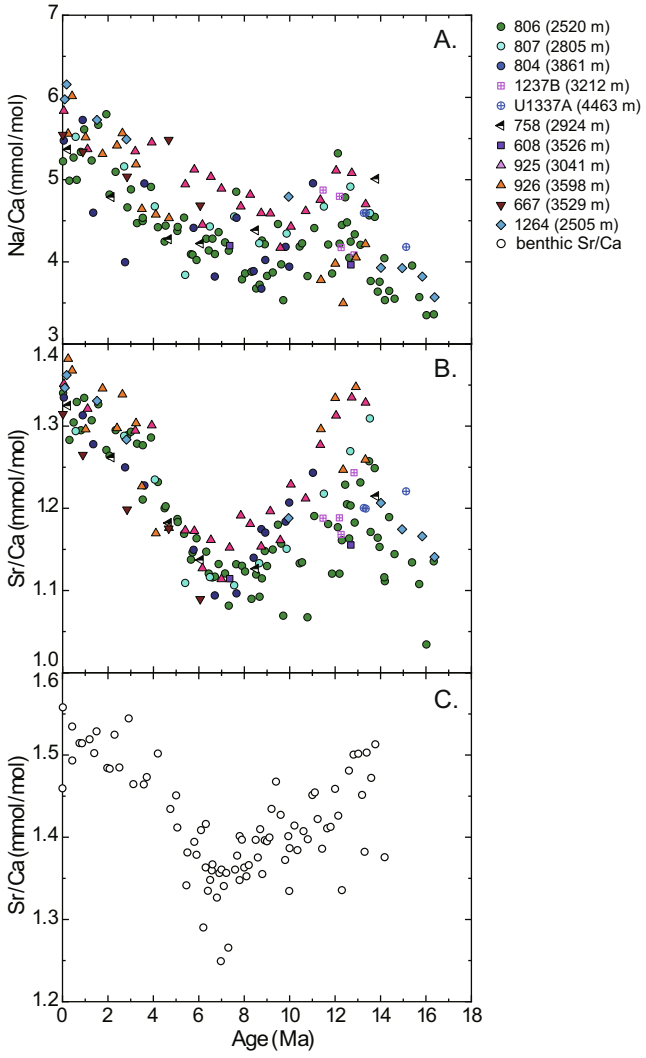

Fig. 4. **Down core foraminiferal Na/Ca and Sr/Ca records.** In A and B, the colored symbols represent Na/Ca and Sr/Ca records in *T. sacculifer* from multiple sites in the Atlantic, Pacific and Indian Oceans, respectively. In C the black open circles represent benthic Sr/Ca records of multiple species normalized to *P. wuellerstorfi* from Lear et al. (2003). The planktic Na/Ca and Sr/Ca records display similar trends over the last 16 Myr, suggesting a common cause such as the long term decrease in seawater [Ca^{2+}] toward present. The similar trends of the planktic and benthic Sr/Ca records and the constant offset between the two records imply that the planktic Sr/Ca records are not impaired significantly by post-depositional alterations, although planktic foraminifera are more susceptible to diagenesis than benthics.

value by 1–3%. The other Na/Ca bands are less enriched in Na than the POS (Bonnin et al., 2019), thus they are less likely to cause great changes in the bulk test Na/Ca values.

Recently, Mezger et al. (2018) reported that Na/Ca ratios measured in foraminifera collected by plankton tows in the Red Sea are notably higher than those observed in core top samples thereby questioning the downcore applicability of an earlier study, based on plankton tow material, reporting a strong Na/Ca-salinity relationship (Mezger et al., 2016). The discrepancy has been attributed to the possible contribution of spines in the tow samples, which are made of calcite enriched in Na, but are quickly lost by dissolution once the tests settle on the seafloor. Unlike plankton tow samples that collect mostly live foraminifera, our cultured specimens underwent gametogenesis and shed their spines in the process. Even if some parts of them were left on the tests, it is unlikely to be the prime cause for substantial enrichments in Na/Ca in our culture samples. While further work should explore the nature of Na enrichments in foraminiferal tests, current studies provide evidence that the Na in secondary phases is preferentially lost during the early stages of diagenesis, and therefore is unlikely to impact the downcore record presented here.

4.2. Culture calibrations

In our culture experiments, the response of planktic foraminiferal Na/Ca and Sr/Ca to changes in seawater [Ca^{2+}] is generally consistent with recent culture experiments on the high-Mg calcitic benthic foraminifer *O. ammonoides* (Hauzer et al., 2018), although the sensitivities of the low-Mg planktic species are lower. In order to accurately

quantify the sensitivities to changes in seawater $[Ca^{2+}]$, however, we first need to assess and correct for other secondary influences, which may be related to changes in salinity and carbonate system parameters.

In this study, temperature is not varied intentionally in the culture experiments. Previous culture experiments with limited data (n = 3) suggest a slightly decreasing trend in *G. ruber* Na/Ca with temperature but an insignificant change in *T. sacculifer* Na/Ca (Allen et al., 2016). Further studies are needed to evaluate the temperature effect on planktic Na/Ca before any robust conclusion can be reached.

The addition of $CaCl_2$ salts in the high $[Ca^{2+}]$ experiments caused a slight increase in salinity of < 1 relative to ambient conditions. It has been previously proposed that foraminiferal Na/Ca increases with salinity (Wit et al., 2013; Mezger et al., 2016), but recent studies have questioned the applicability of these observations to downcore records (e.g., Allen et al., 2016; Hauzer et al., 2018; Mezger et al., 2018). The sensitivity of foraminiferal Na/Ca to salinity changes is a matter of ongoing debate beyond the scope of this paper, and can be found elsewhere (Allen et al., 2016; Mezger et al., 2016; Bertlich et al., 2018; Mezger et al., 2018). However, even if we apply the highest sensitivity to our culture results, an increase of 1 salinity unit would only lead to an increase in Na/Ca of ~0.1 mmol/mol, which is much smaller than our observed influence of seawater $[Ca^{2+}]$ and should at most have a negligible influence on the culture calibrations.

In experiments that contain 20 mmol/kg $[Ca^{2+}]$, the carbonate chemistry was also modified, thus complicating the responses of trace elements contents in foraminifera to $[Ca^{2+}]$. Previous culture experiments examined the dependence of Na/Ca and Sr/Ca on changes in solution $[CO_3^{2-}]$ with modern $[Ca^{2+}]$ and $[Mg^{2+}]$ (Allen et al., 2016). Here we formulate the relationship as a function of the calcite saturation ($\Omega_{calcite}$) to account for the fact that both $[Ca^{2+}]$ and $[CO_3^{2-}]$ are changing in our experiments and over geologic times. This is important to test because calcite saturation controls crystal growth rate, which in turn can influence the incorporation of trace elements into the inorganic precipitates (Watson, 1996). Using data from the pH experiments on *G. ruber* and *T. sacculifer* of Allen et al. (2016), we quantify the influence of $\Omega_{calcite}$ on $(Na/Ca)_{test}$ and $(Sr/Ca)_{test}$ at modern seawater $[Ca^{2+}]$. Because the ranges of $\Omega_{calcite}$, $(Na/Ca)_{test}$ and $(Sr/Ca)_{test}$ for the two foraminiferal species may show inter-species difference, we calculate the average values for $\Omega_{calcite}$, $(Na/Ca)_{test}$, and $(Sr/Ca)_{test}$ in each species, and normalize the data by subtracting the corresponding average values. Given the similarity of the pH effects on *G. ruber* and *T. sacculifer*, we then combine the normalized data from the two species. The normalized data suggest $(Na/Ca)_{test}$ increases by 0.067 ± 0.011 mmol/mol per unit change in $\Omega_{calcite}$ ($R^2 = 0.80$, $p = 0.0002$; Table S5, Fig. 2C), but the correlation for $(Sr/Ca)_{test}$ is much weaker (slope = 0.007 ± 0.003, $R^2 = 0.26$, $p = 0.0175$; Table S5, Fig. 2D). We use these relationships to correct foraminiferal Na/Ca from our culture experiments for the variability in carbonate system parameters. Foraminiferal Na/Ca data are normalized to $\Omega_{calcite}$ equaling 6, which is close to the modern sea surface value. Applying these corrections to the Na/Ca data yields the Na/Ca sensitivity to changes in dissolved $[Ca^{2+}]_{SW}$ for each species:

G. ruber $(Na/Ca)_{test} = 3.96 \pm 0.45 + 0.072 \pm 0.010 \cdot (Na/Ca)_{SW}$ ($R^2 = 0.82$)
T. sacculifer $(Na/Ca)_{test} = 2.68 \pm 0.30 + 0.075 \pm 0.010 \cdot (Na/Ca)_{SW}$ ($R^2 = 0.79$)
O. universa $(Na/Ca)_{test} = 2.47 \pm 0.14 + 0.072 \pm 0.004 \cdot (Na/Ca)_{SW}$ ($R^2 = 0.91$)

where $(Na/Ca)_{SW}$ ratios are in mol/mol (Fig. 5A). The calibration for *T. sacculifer*, the species we are using for the down core reconstruction, is not significantly different from the pooled sensitivity for the three species:

$$\Delta(Na/Ca)_{test} = 0.073 \pm 0.002 \cdot \Delta(Na/Ca)_{SW};\ (R^2 = 0.84)$$

Given a non-zero intercept, Hauzer et al. (2018) suggested using a distribution function between Na/Ca in the test and that in the solution defined by a power function $y = a \cdot x^H$, where y is Na/Ca in the test, x is Na/Ca in the solution, and a and H are constants obtained from the power curve fit to the experimental data. This equation follows the formulation previously suggested to account for the effect of changes in seawater Mg/Ca on foraminiferal Mg/Ca (Segev and Erez, 2006; Hasiuk and Lohmann, 2010; Evans and Müller, 2012). For comparison with the linear functions, we calculate the following power functions for the three species with 1 SD uncertainty based on the corrected data:

G. ruber $(Na/Ca)_{test} = 1.74 \pm 0.42 \cdot (Na/Ca)_{SW}^{0.373 \pm 0.069}$ ($R^2 = 0.83$)
T. sacculifer $(Na/Ca)_{test} = 0.98 \pm 0.20 \cdot (Na/Ca)_{SW}^{0.478 \pm 0.060}$ ($R^2 = 0.79$)
O. universa $(Na/Ca)_{test} = 0.89 \pm 0.08 \cdot (Na/Ca)_{SW}^{0.490 \pm 0.027}$ ($R^2 = 0.92$)

In contrast with Na/Ca that has non-zero intercepts, the regressions for Sr/Ca go through the origin within uncertainty, implying that the distribution coefficients of Sr in these planktic foraminiferal species are independent of the Sr/Ca in the solutions (Fig. 2B). The multispecies regression suggests a distribution coefficient of $D_{Sr} = 0.16 \pm 0.02$ ($R^2 = 0.99$), which is higher than observed for inorganic calcites (Mucci and Morse, 1983; Elderfield, 1996) but in agreement with other culture experiments performed under changing $[Sr^{2+}]_{SW}$ and constant $[Ca^{2+}]_{SW}$ ($D_{Sr} = 0.17 \pm 0.03$; Delaney et al., 1985) or under changing Sr/Ca of the growth medium ($D_{Sr} = 0.16 \pm 0.01$; Allen et al., 2016).

In summary, the culture results of the three planktic species support the hypothesis that changes in the elemental compositions of Na and Sr in the tests, vary proportionally to changes in seawater $[Ca^{2+}]$ concentrations. In the following sections we primarily focus on the utility of Na/Ca in *T. sacculifer* as a potential proxy for reconstructing paleo-seawater $[Ca^{2+}]$.

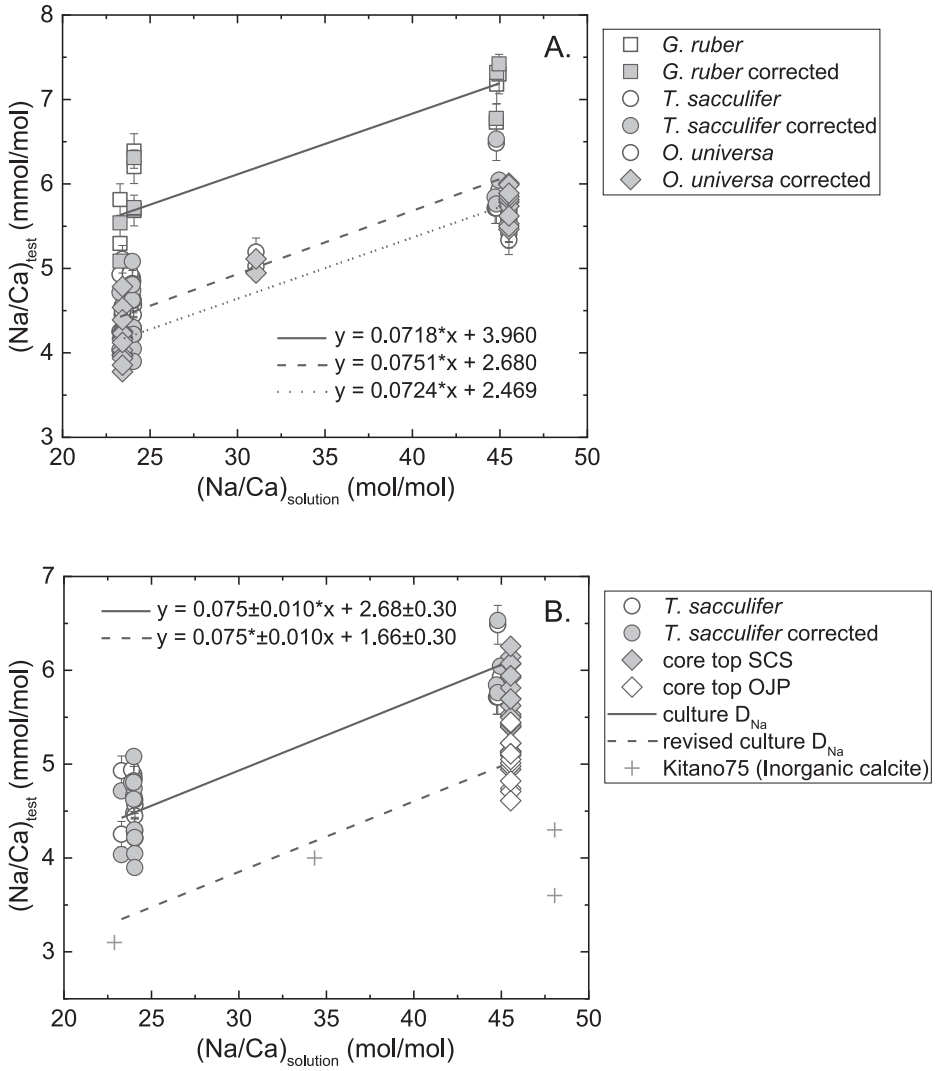

Fig. 5. **Distribution coefficients of Na (D_{Na}) in planktic foraminifera.** A shows the culture experiment results on three planktic species. Na/Ca in *G. ruber*, *T. sacculifer*, and *O. universa* (open symbols) and that after correcting for $\Omega_{calcite}$ effects (closed symbols; correction referring to Fig. 2C) are plotted with Na/Ca in the culture solutions. Linear regression is performed for each species. B displays the D_{Na} for *T. sacculifer* in the down core sediments. The uncorrected (open circles) and the $\Omega_{calcite}$-corrected Na/Ca (filled circles) in *T. sacculifer* from the culture experiments are both plotted, and linear regression (solid line) is performed on the corrected Na/Ca data. Core top Na/Ca data from the Ontong Java Plateau (open diamonds) and the South China Sea (filled diamonds) and Na/Ca data from the inorganic calcite growth experiments (plus symbols; Kitano et al., 1975) are also plotted for comparison. The regression line based on the corrected Na/Ca data from the culture experiments is shifted down by 1.02 mmol/mol to reflect the offset between the average of the culture experiments data at modern ocean Na/Ca value and the average of the core top data from the Ontong Java Plateau. The new regression is represented by a dashed line, which is used for reconstructing seawater [Ca^{2+}] from the down core *T. sacculifer* Na/Ca records. For details in statistical analysis, please refer to Table S5. (For interpretation of the references to colour in this figure legend, the reader is referred to the web version of this article.)

4.3. Dissolution effects on core top foraminiferal Na/Ca records

Na/Ca and Sr/Ca in the tests of *T. sacculifer* from core top samples along bathymetric transects in the South China Sea (SCS) and Ontong Java Plateau (OJP) decrease with increasing water depth, concomitant with the decrease in the average test weight (Fig. 3). The decreasing trends in these elemental concentrations are attributed to post-depositional dissolution as previously proposed to explain the loss in Mg/Ca (e.g., Brown & Elderfield, 1996; Johnstone et al., 2016; Rosenthal et al., 2000; Rosenthal & Lohmann, 2002; Sadekov et al., 2010). Mineralogical studies on inorganically precipitated calcite suggest that at low [Sr^{2+}] of the solution, Sr^{2+} substitutes Ca^{2+} in the calcite lattice (Tesoriero and Pankow, 1996; Parkman et al., 1998; Gabitov and Watson, 2006). Assuming that these results also apply to foraminiferal calcite (based on the similarity in distribution coefficients), it is reasonable to assume that the depth-related decrease in core tops Sr/Ca is due to preferential dissolution of parts of the calcitic test enriched in trace elements including Mg, Sr and likely Na rather

than a loss from interstitial sites or other phases. The strong covariance between the trends in the core tops and down core Na/Ca and Sr/Ca suggests that the distribution of Na^+ in the calcitic test may be mechanistically linked to that of Sr^{2+} (Figs. 3 and 4).

Statistical analysis on the correlations of Na/Ca and Sr/Ca with $\Omega_{calcite}$ supports our inference above that the decreases in Na/Ca and Sr/Ca are due to dissolution. The core tops planktic Na/Ca decreases with decreasing seawater $\Omega_{calcite}$ at a rate of 1.90 ± 0.21 mmol/mol per unit change in $\Omega_{calcite}$ (Table S5, Fig. S3A). The Sr/Ca also decreases with decreasing $\Omega_{calcite}$, but there are offsets between the two sets of Sr/Ca data from the SCS and OJP at the same $\Omega_{calcite}$, and the correlations seem to be slightly different from the two regions (Table S5, Fig. S3B), suggesting that Sr/Ca may respond to other hydrographic variables indirectly such as pressure rather than $\Omega_{calcite}$.

The relationships between foraminiferal Na/Ca and Sr/Ca in the core top and down core *T. sacculifer* tests are statistically similar, i.e., the slopes are 7.17 ± 2.60 and 5.62 ± 0.43, respectively (Table S5, Fig. S4), implying that either the downcore records solely reflect dissolution, or that the incorporation of Na and Sr into the test and diagenetic removal of them from foraminiferal calcite are tightly coupled. However, several lines of evidence suggest that the down core records are not dominated by dissolution effect. First, neither Sr/Ca nor Na/Ca decreases monotonically with sediment depth as could be expected based on the core top trends. Additionally, the Na/Ca and Sr/Ca maxima in the down core records occur at different sediment depths at different sites but are contemporaneous (Figs. 4 and S5). The large changes in both ratios occur at relatively shallow burial depth (<250 mbsf), but the SEM photos of foraminifera and coccolithophores show no major signs of dissolution or recrystallization through this interval (Appendix A). Moreover, the down core planktic Sr/Ca compilation exhibits a similar trend to the records from benthic foraminifera (Lear et al., 2003), increasing from 16 to 12–14 Ma, reaching a local high, then decreasing to ~ 8 Ma, and finally increasing toward the present (Fig. 4-B-C). Remarkably, the offset between the planktic and benthic Sr/Ca records, which are based on multiple benthic species, is relatively constant throughout the entire time period. Given the different susceptibility of benthic and planktic tests to dissolution and the constant interspecies offsets, it seems that a strong dissolution overprint is unlikely the primary cause of the down core changes in Sr/Ca.

Finally, we note that the Na/Ca in the culture experiments is higher than that in both the core top and down core samples, showing a weaker relationship (lower slope) with Sr/Ca (Table S5, Fig. S4). The similar slopes of the core top and down core records suggest that $[Sr^{2+}]_{SW}$ should not have played a significant role, otherwise the two slopes would have been more different (Fig. S4). This is also supported by the similar magnitudes of the long-term variations in down core Na/Ca and Sr/Ca records (Fig. 4). Therefore, the difference between the culture and the fossil records may be due to the occurrence of additional phases enriched with Na in fresh foraminiferal tests, that are likely lost soon after deposition on the seafloor. As is discussed in Section 4.1, preferential losses of Na-enriched bands within foraminiferal tests should not cause a significant change in the bulk test Na/Ca. Alternatively, the enriched Na may also be related to high carbonate saturation state in the culture experiments (Haynes et al., 2019), similar to Li/Ca and Sr/Ca, which have higher distribution coefficients in calcite when the crystal growth rate is driven by high omega values (Tang et al., 2008; Füger et al., 2019). In the following sections, we discuss the effects of dissolution and recrystallization on the down core Na/Ca records.

4.4. Dissolution effects on down core planktic Na/Ca records

We note that the down core Na/Ca records from Pacific sites are generally lower than those from Atlantic sites during the same time intervals, and we attribute the offset to greater dissolution effects at the Pacific sites. Therefore, we correct for dissolution effects on down core Na/Ca records at each site, using the slope of 1.90 ± 0.21 mmol/mol per unit difference in modern ocean $\Omega_{calcite}$ (Table S5, Fig. S3A) between each site and Site 806, where the $\Omega_{calcite}$ is close to unity and the temporal range is the widest among all the sites. Given that core top Na/Ca values at specific $\Omega_{calcite}$ values vary by up to 0.4 mmol/mol (Fig. S3A), the $\Omega_{calcite}$ difference that is less than 0.2 unit may not be distinguished from the inherent variability in Na/Ca values. Therefore, only the sites with $\Omega_{calcite}$ values higher by 0.2 unit than that at Site 806 are corrected, including all the five sites from the Atlantic Ocean. Sites 804 and U1337 are both located in regions with highly undersaturated seawater, and the Na/Ca records from these two sites may have been influenced dramatically due to dissolution. Therefore, they are excluded from the compilation of the down core Na/Ca records in Fig. 6.

Alternatively, we assess the possibility that the difference between the Pacific and Atlantic sites is due to salinity difference. The sea surface salinities at Atlantic sites are on average 1.01 ± 0.16 higher than that at Site 806 (Table S1). Using a sensitivity of 0.115 mmol/mol Na/Ca per unit change in salinity (Bertlich et al., 2018), this translates to a salinity effect of 0.12 ± 0.02 mmol/mol on Atlantic data. This is less than one fourth of the dissolution effect, which is 0.53 ± 0.16 mmol/mol on average. Therefore, the difference between the Pacific and Atlantic sites is more likely due to the dissolution effect than the salinity effect.

The dissolution-corrected down core Na/Ca records from different sites are more consistent with each other than before the correction (Fig. 6). The Na/Ca records from the Atlantic Ocean are lowered to various extents because the bottom water in the Atlantic is generally more saturated than in the Pacific Ocean at present. Notably, the long-term trend is retained after the correction, exhibiting an increasing trend toward present with a local high between 12 and 13 Ma (Fig. 6), suggesting that the down core Na/Ca records are not severely compromised by carbonate dissolution.

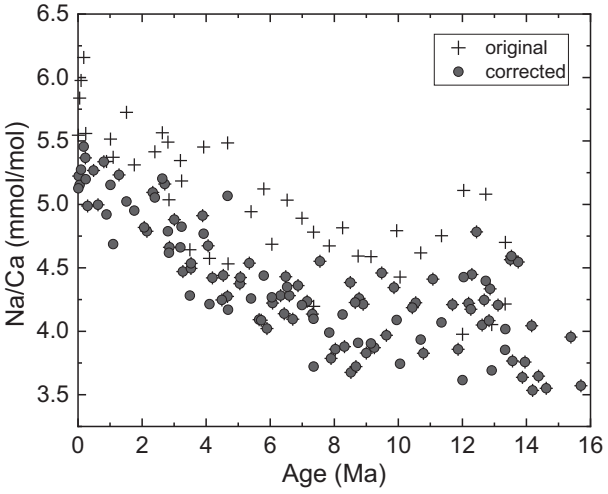

Fig. 6. **Down core Na/Ca data correcting for the $\Omega_{calcite}$ effect.** Because the $\Omega_{calcite}$ at ODP Site 806 is close to unity, the down core Na/Ca records from other sites (Fig. 4A) are normalized to this site, correcting for the $\Omega_{calcite}$ effect displayed in Fig. S3A. For details on the correction, please refer to Section 4.4. The uncorrected and corrected data are represented by plus signs and filled circles, respectively. Largely, Na/Ca records from the Atlantic sites are lowered, lowering the average value of the corrected Na/Ca data from all sites.

4.5. Recrystallization effects on down core planktic Na/Ca records

In down core sediments, foraminiferal tests are susceptible not only to dissolution, but also to recrystallization of the primary test and precipitation of secondary overgrowth of $CaCO_3$ from the pore water. Here we use the numerical model developed by Fantle and DePaolo (2006) to estimate the effect of recrystallization on down core *T. sacculifer* Na/Ca records. A full discussion of the implementation of the model is given in appendix B below. The following provides a summary of the procedure. In Fantle and DePaolo (2006), the time-dependent recrystallization rate ($R = \alpha + \beta e^{-time/\gamma}$) of the bulk carbonate is derived by the model using down core Sr/Ca and Sr isotope data from ODP Site 807. The variable "time" in R is the time in Myr that passed since the sediment deposition rather than its absolute age, suggesting that recrystallization decreases exponentially with deposition time. We adopted the R ($=0.035*e^{-time/11}$) used in Fantle and DePaolo (2006) to assess implications to the down core foraminiferal Na/Ca records at Sites 807 and 806 on the Ontong Java Plateau, where the down core data range over the last 16 Myr.

Assuming the recrystallization rate of the bulk carbonate follows the function $R = 0.035*e^{-time/11}$, then a maximum of 30% of the bulk carbonate would have been recrystallized over the last 16 Myr. In addition, because nannofossil ooze dominates the carbonate sediment in this study (Si and Rosenthal, 2019), recrystallization should have mostly happened on coccolithophores rather than foraminifera. Considering that initial recrystallization of the surface of carbonate could impede subsequent recrystallization of the inner layers (Honjo and Erez, 1978), the fraction of recrystallized carbonate in the real condition should be smaller than we estimated.

To assess the impact of recrystallization on the down core Na/Ca record we test the hypothesis that over the past 16 Myr, seawater Na/Ca did not change (i.e., seawater $[Ca^{2+}]$ was constant) and therefore the pristine value of foraminiferal Na/Ca should have also been constant through time at the core top value (the dashed lines in Fig. S6). Based on this hypothesis, down core changes in foraminiferal Na/Ca are modeled. The deviation of the modeled result from the core top value should reflect diagenetic effects (the solid lines in Fig. S6). Because no core top value is available at the water depths of the two sites, the pristine value of foraminiferal Na/Ca is set to the value of the youngest sample that is available at each site, both of which are younger than 1 Ma.

The modeled Na/Ca profiles display different trends than the measured data, showing monotonic decreasing trends that are significantly smaller than the changes in measured data. In turn, the results suggest that recrystallization cannot fully explain the down core variations in foraminiferal Na/Ca (Fig. S6). Recrystallization effects increase with sediment depth, but the maximum effect at the depth is less than 3%, suggesting that most of the variations in the down core Na/Ca reflect changes in seawater $[Ca^{2+}]$ rather than recrystallization. We note, however, that this estimate is sensitive to the choice of distribution coefficient of Na into the recrystallized calcite. We discuss the influence of recrystallization on the reconstructed seawater $[Ca^{2+}]$ in the next section.

Several lines of evidence corroborate the inference derived from the model results that the down core planktic records of Na/Ca are not strongly compromised by recrystallization or calcite overgrowth. The study of Pearson et al. (2001) shows that the $\delta^{18}O$ of planktic foraminifera from Eocene sediments is strongly biased by diagenesis, suggesting that about 50% of the test can be recrystallized. Similarly, using secondary ion mass spectrometry (SIMS), Kozdon et al. (2013) report about 50% of the test of planktic foraminifera from the PETM (~56 Ma) sediments is affected by diagenesis. Both studies support their conclusions with scanning electron microscope (SEM) pictures showing strong evidence for inorganically precipitated crystals. In contrast, our samples are much younger and come from shallower burial depths with presumably less diagenetic overprint as suggested by the model results. SEM inspection of the foraminiferal tests from our down core records shows a high degree of preservation with no clear evidence of recrystallized or secondary precipitates (Appendix A1), as seen in the older samples. Furthermore, there is no evidence for significant calcite or dolomite overgrowth on cocoliths from these samples, suggesting minimum secondary precipitation (Appendix A2). A close look at the wall-structure of *T. sacculifer* test, however, shows signs of dissolution in Miocene samples especially from Pacific cores (Appendix A3). Overall, we conclude that the primary geochemical signals are preserved in these samples, despite some diagenetic overprint, which is discussed above.

5. PALEOCEANOGRAPHIC IMPLICATIONS FOR DOWN CORE PLANKTIC NA/CA RECORDS

As discussed above, based on the similarity between the Na/Ca and Sr/Ca records for the past 16 Myr (Fig. 4) and our assessment of the diagenetic effects, including dissolution of primary test calcite or recrystallization, we argue that the down core records primarily reflect changes in seawater composition during the past 16 Myr. To interpret the down core records in terms of changes in $[Ca^{2+}]_{SW}$, we first estimate the partition coefficient of Na (D_{Na}) in the foraminiferal calcite of *T. sacculifer*. Although we displayed the power functions in Section 4.2, given the limited available dataset for *T. sacculifer*, we prefer to use the linear equation at the moment. The Na/Ca values in the core top and down core samples are generally lower than those from the culture experiments under modern $[Ca^{2+}]_{SW}$ conditions (Fig. S4), which is likely due to the loss of Na phases that are only present in live specimens (see Section 4.1). Therefore, we adopt the same slope from the culture calibration for *T. sacculifer* but adjusted the intercept by –1.02 mmol/mol, which is the difference between the average $\Omega_{calcite}$-corrected Na/Ca from the culture experiments under modern $[Ca^{2+}]$ conditions and the average Na/Ca from the core top samples on the Ontong Java Plateau. The corrected regression, which was applied to the down core Na/Ca records to reconstruct paleo-$[Ca^{2+}]_{SW}$ yields the following equation:

$$(Na/Ca)_{test} = 1.66 \pm 0.30 + 0.075 \pm 0.010 \cdot (Na/Ca)_{SW}\ ; \quad (R^2 = 0.79;\ \text{Fig. 5B})$$

Due to its very long residence time in the ocean, the seawater $[Na^+]$ during the past 16 Myr was most likely the same as at present. Based on the results from the culture experiments, we posit that the observed down core decrease in foraminiferal Na/Ca is dominantly due to progressively higher seawater $[Ca^{2+}]$ concentration in the past. In our reconstruction, we do not correct for any changes in surface saturation state through time, because although seawater $[Ca^{2+}]$ likely changed, $[CO_3^{2-}]$ also likely changed in tandem to maintain a constant saturation state (Zeebe and Tyrrell 2019). We estimate the changes in $[Ca^{2+}]_{SW}$ using the culture calibration suggested above (Figs. 5 and 7) with uncertainties from Na/Ca measurement, the estimate of D_{Na}, diagenesis, and data smoothing. To consider the diagenetic effects on reconstructed $[Ca^{2+}]_{SW}$, we derive the difference between the modeled result and the "core top" value at Site 806 (Fig. S6) and assume other sites have gone through similar diagenetic processes. This uncertainty is added to the analytical error, the total of which counted as uncertainties associated with Na/Ca data. The results suggest that the uncertainty due to diagenetic effects on the reconstructed $[Ca^{2+}]_{SW}$ is comparable, though lower than the uncertainty associated with the calibration (Fig. 7).

The reconstructed $[Ca^{2+}]_{SW}$ displays a generally decreasing trend from 16 Ma toward the present, except for a local high between 8 and 9 Ma. Our $[Ca^{2+}]_{SW}$ record is consistent with the fluid inclusion estimates available for the past 16 Myr (Horita et al., 2002; Brennan et al., 2013), which also suggest much higher $[Ca^{2+}]_{SW}$ in the Miocene and Pliocene than in recent. However, this study not only offers independent validation to the fluid inclusion results but also provides a $[Ca^{2+}]_{SW}$ record at the sub-million-year temporal resolution, comparable with other Neogene paleoceanographic and climatic records such as the benthic foraminiferal $\delta^{18}O$ records.

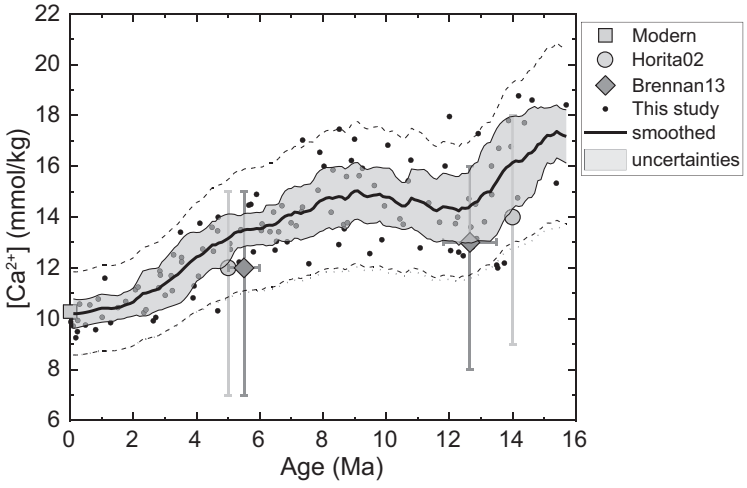

Fig. 7. **Reconstructed $[Ca^{2+}]_{SW}$ from down core planktic foraminiferal Na/Ca records at multiple sites.** $[Ca^{2+}]_{SW}$ is reconstructed from the corrected down core Na/Ca records (Fig. 6) using the adjusted D_{Na} based on culture experiment results (Fig. 5B), plotted as black dots. The values are interpolated to evenly-spaced ages at a temporal resolution of 0.1 Ma and then smoothed by 25-point moving average, displayed as the thick line. Uncertainties (grey shadings and dashed lines) are estimated for the reconstructed $[Ca^{2+}]_{SW}$, with the thin line representing uncertainties associated with the data smoothing, the dashed lines representing uncertainties from Na/Ca measurement and D_{Na} calibrations, and the dotted line including recrystallization effect on top of the lower dashed line. Fluid inclusion records (light grey diamonds and dark grey circles) with uncertainties and modern ocean value (square) are plotted for comparison. The $[Ca^{2+}]_{SW}$ based on planktic Na/Ca generally complies with the other records. Furthermore, it provides a continuous high-resolution record. (For interpretation of the references to colour in this figure legend, the reader is referred to the web version of this article.)

6. SUMMARY AND CONCLUSIONS

This study presents the results of culture experiments with planktic foraminifera as a proof of concept for the interpretation of planktic foraminiferal Na/Ca records, in terms of long-term changes in seawater calcium concentration ($[Ca^{2+}]_{SW}$). The new culturing data confirm earlier results from culturing of the benthic foraminifer *Operculina ammonoides* (Hauzer et al., 2018), both showing that Na/Ca is negatively correlated to $[Ca^{2+}]_{SW}$. Our study also agrees with the benthic study in that foraminiferal Na/Ca is weakly correlated with calcite saturation state ($\Omega_{calcite}$) during shell formation. As we assume the surface water $\Omega_{calcite}$ was relatively constant throughout the Cenozoic Era (Zeebe and Tyrell, 2019), we did not consider that effect on the down core foraminiferal Na/Ca records but instead assess the effects of possible shell dissolution and recrystallization in the sediment column. Core top data of *Trilobatus sacculifer* show similar decreasing trends in foraminiferal Na/Ca and Sr/Ca with water depth due to the dissolution of their tests as indicated by the concomitant decrease in the average test weight. The strong covariance with Sr is consistent with a recent study suggesting substitution of Na^+ for Ca^{2+} sites in the lattice structures (Yoshimura et al., 2017). After considering the effects of temperature, salinity and diagenetic alteration, we conclude that the down core decrease in Na/Ca, which parallels the trend in Sr/Ca and is observed at multiple ocean sites, most likely reflects changes in $[Ca^{2+}]_{SW}$. Based on the calibrations generated in this study, our down core planktic Na/Ca record suggests 46 ± 22% higher $[Ca^{2+}]_{SW}$ in the mid-Miocene (11.6–16.0 Ma) than at present, with most of the change occurring at the mid-Miocene and since the beginning of the Pliocene. Our $[Ca^{2+}]_{SW}$ record is different from the results based on Ca isotopes in that the other records suggest $[Ca^{2+}]_{SW}$ increased from the early Miocene to ~ 12 Ma, but our record suggests $[Ca^{2+}]_{SW}$ decreased continuously from the mid-Miocene toward the present. The range of our reconstructed $[Ca^{2+}]_{SW}$ is generally consistent with the records derived from fluid inclusions, displaying an offset of ~ 1 mmol/kg within uncertainty, which adds confidence to both reconstructions. Foraminiferal Na/Ca offers a new method for generating a temporally continuous record of seawater calcium concentration and much higher resolution than offered by the fluid inclusion data. The new $[Ca^{2+}]_{SW}$ reconstruction shows resemblance with Neogene climate-related records (e.g., the benthic foraminiferal $\delta^{18}O$ records), which likely reflects on the causes of changes in seawater chemistry by point-to-point comparison. We note, however, that at this point it would be important to confirm our planktic foraminiferal record with other independent reconstructions, such as using benthic foraminifera.

AUTHOR CONTRIBUTIONS

Y.R. and J.E. conceived the idea of using foraminiferal Na/Ca as a proxy for seawater Ca concentration. L.H. and B.H. performed the culture experiments on planktic foraminifera and together with Y.R. they analyzed Na/Ca and Sr/Ca in cultured foraminifera. X.Z., Y.R., and K.H. analyzed Na/Ca and Sr/Ca in core top and down core samples. All the authors contributed to the writing of the manuscript.

Declaration of Competing Interest

The authors declare that they have no known competing financial interests or personal relationships that could have appeared to influence the work reported in this paper.

ACKNOWLEDGEMENTS

X. Z. and Y. R. acknowledge IODP for providing samples for this study, Kaixuan Bu for his assistance in trace element analysis. This work was funded by NSF OCE-BSF-1634573 to Y. R., NSF-BSF grant 2016534 to J. E. and Y. R., and NSF OCE 12-32987 to B. H. We thank Stephen Eggins and Katherine Holland for providing seawater composition data for the culture experiments on planktic foraminifera. We also thank for Toshihiro Yoshimura and other four anonymous reviewers' comments. All the data will be available on NOAA's website.

APPENDIX A. SEM PHOTOS OF FORAMINIFERA AND COCCOLITHOPHORES

Plate A1. SEM photos of test walls of down core *T. sacculifer* from Sites 806, 1237, and 925. The photos show high degree of preservation with no strong evidence of recrystallization. Sample labels are as follows: A. Site 806B, 1H1, 41–45 cm, 0.02 Ma; B: Site 925B, 1H2, 50–52 cm, 0.05 Ma; C. Site 806B, 55X2, 80–85 cm, 14.62 Ma; D. Site 925B, 17H2, 47–49 cm, 5.40 Ma; E. Site 1237B, 21H2, 101–103 cm, 12.19 Ma; F. Site 925B, 27H2, 50–52 cm, 9.58 Ma.

Plate A2. SEM photos of nannofossils from down core sites 806 and 1264. The photos show minimum secondary precipitation on the nannofossils. Sample labels are as follows: A. Site 806B, 3H1, 53–54 cm, 0.81 Ma; B. Site 1264B, 1H1, 89 cm, 0.18 Ma; C. Site 806B, 10H1, 49–50 cm, 3.53 Ma; D. Site 1264B, 8H3, 50 cm, 5.65 Ma; E. Site 806B, 39X4, 61 cm, 10.44 Ma; F. Site 1264B, 20H1, 48 cm, 15.84 Ma.

Plate A3. SEM photos of the cross sections of *T. sacculifer* tests from core top site MW91-9 (OJP) and down core sites 806, 1237, and 925. The photos show good preservation of the younger samples but signs of dissolution in older samples. Sample labels are as follows: A. MW91-9, GGC-15, 5–6 cm, 2311 m in water depth; B. Site 925B, 1H2, 50–52 cm, 0.05 Ma; C. Site 806B, 1H1, 41–45 cm, 0.02 Ma; D. Site 925B, 17H2, 47–49 cm, 5.40 Ma; E. Site 1237B, 21H2, 101–103 cm, 12.19 Ma; F. Site 925B, 27H2, 50–52 cm, 9.58 Ma.

APPENDIX B. DIAGENETIC MODEL

B.1. Estimating the recrystallization rates (*R*)

The depositional diffusion–reaction model that we adopted in this study is described in detail in Fantle and DePaolo (2006). Parameters in this model are varied to fit the pore water $[Sr^{2+}]$ and $^{87}Sr/^{86}Sr$ records. The evolution

of the concentration of an element in pore water (C_f) and sediments (C_s) are described by general diagenetic equations as follows:

$$\frac{\partial C_f}{\partial t} = DI\frac{\partial^2 C_f}{\partial z^2} - v\frac{\partial C_f}{\partial z} + RM(C_s - KC_f) \quad (1)$$

$$\frac{\partial C_s}{\partial t} = -V\frac{\partial C_s}{\partial z} - R(C_s - KC_f) \quad (2)$$

where DI is the diffusion coefficient of the element in the pore water in m^2/Myr, v is the advection velocity in m/Myr, V is the compaction velocity in m/Myr due to sediment accumulation, R is the recrystallization rate in 1/Myr, M ($=\rho_s(1-\phi)/\rho_f\phi$) is the local solid/fluid mass wratio, and K is the equilibrium distribution coefficient of the element between the solid and the fluid. As discussed in Fantle and DePaolo (2006) for Sr, DI_{Sr} is 7500 m^2/Myr, and K_{Sr} scales with pore water Ca concentration, with the highest K_{Sr} equaling 20.5 at the basalt-sediment interface and decreasing upward as pore water [Ca^{2+}] decreases. The spatial framework is defined as $z = 0$ at the basalt-sediment interface and z is positive upward.

After solving Eq. (1) using a modified centered finite difference approach, the evolution of an isotope i in the fluid is described as follows:

$$\frac{C_{if_j}^{n+1} - C_{if_j}^{n-1}}{2\Delta t} = \frac{DI_s}{(\Delta t)^2}\left[C_{if_{j+1}}^{n} + C_{if_{j-1}}^{n} - C_{if_j}^{n+1} - C_{if_j}^{n-1}\right] - v \times \frac{C_{if_{j+1}}^{n} - C_{if_{j-1}}^{n}}{2\Delta z} + R_j M_j[C_{is_j}^{n-1} - KC_{if_j}^{n-1}] \quad (3)$$

where we solve for $C_{if_j}^{n+1}$ and f and s stand for fluid and solid, respectively, n and j stand for the temporal and spatial grid, respectively, and i refers to ^{86}Sr or ^{87}Sr. As in Fantle and DePaolo (2006), we set the grid spacing Δz as 25 meters and the time step Δt as 0.025 Myr, so that the stability requirement for the model is met. The advection velocity v and compaction rate V are set to zero for simplification, as advection due to compaction is insignificant (Richter, 1993). Previous studies have suggested that the recrystallization rate (R in 1/Myr), which is the estimate of the fraction of carbonate that is recrystallized every million years, is highest right after deposition and decreases rapidly with deposition time (Richter and DePaolo, 1987; Richter and Liang, 1993; Fantle and DePaolo, 2006). Therefore, following Fantle and DePaolo (2006), R is described as a function of deposition age by an exponential equation constrained by three variables (α, β, γ) as follows:

$$R = \alpha + \beta e^{-time/\gamma} \quad (4)$$

where "time" is the time in Myr that passed since the sediment deposition rather than its absolute age, implying that the down core profile of R is the same at any geologic time that is discussed in this study (see the solid lines in Fig. 5b and e in Fantle and DePaolo (2006)). The content of ^{86}Sr in the solids is assumed constant at 9.86% of the mean value of the Sr content in the down core sediments in accord with its natural abundance (Richter and DePaolo, 1987). Likewise, the concentration of ^{86}Sr in the seawater-pore water interface is held constant at 9.0 μmol/kg throughout the modeled time interval. The content of ^{87}Sr in the solids and the concentration of ^{87}Sr in the pore water at the seawater-pore water interface are calculated by multiplying the content or concentration of ^{86}Sr and the $^{87}Sr/^{86}Sr$ record of the sediment or pore water, respectively. When the down core $^{87}Sr/^{86}Sr$ data are unavailable from our target sites, values from the global $^{87}Sr/^{86}Sr$ curve were adopted (Hess et al., 1986; Richter and DePaolo, 1988; Hess et al., 1989). The Sr concentration and isotopic data in pore waters and sediments at Sites 807 and 806 are from published literature (Shipboard Scientific Party, 1991; Fantle and DePaolo, 2006). Because the Sr content in bulk sediment at these two sites does not display any obvious trends at either site, it is assumed constant throughout the sediment column.

The best fit of the modeled result to the measured data is determined by minimizing the relative difference between the model and the data. As described in Fantle and DePaolo (2006), the best fit yields $R = 0.035*e^{-time/11}$ for Site 807, which is adopted in the next step to assess recrystallization effect on the down core Na/Ca at Sites 807 and 806.

B.2. Recrystallization effect on Na/Ca

Pore water [Na^+] and foraminiferal Na/Ca are modeled using the R estimated by fitting the Sr concentration and isotopic composition as in Fantle and DePaolo (2006). Solving Eq. (2) using finite difference approach yields the solution describing the evolution of an isotope i in the solid as follows:

$$\frac{C_{is_j}^{n+1} - C_{is_j}^{n-1}}{2\Delta t} = -R_j[C_{is_j}^{n-1} - KC_{if_j}^{n-1}] \quad (4)$$

where we solve for $C_{is_j}^{n+1}$. The diffusion coefficient of Na in the pore water (DI_{Na}) is estimated to be 11875 m^2/Myr for the down core sediments (Li and Gregory, 1974; Berner, 1980). Previous inorganic $CaCO_3$ precipitation experiments suggest that the partition coefficient K_{Na} averages at 0.091 ± 0.013 (Kitano et al., 1975; Busenberg and Plummer, 1985; Kawabata et al., 2021). M is the same as in the model for Sr. C_s at the sediment-rock interface is set to the Na content in *T. sacculifer* of the shallowest depth that is available at each site. Once the pore water [Na^+] in the upper and lower boundary of the sediment column is given, the evolution of [Na^+] in the pore water and carbonate can be solved through Eqs. (3) and (4).

When constant seawater [Na^+] is used as the upper boundary condition through time, the modeled pore water [Na^+] is too low and the down core trend is opposite to that of the measured values. We suppose such a mismatch of the model and the data likely reflects additional Na sources to the pore water other than the dissolution of foraminiferal tests. Given its long residence time, it is unlikely that seawater [Na^+] has decreased significantly from early Neogene to present. Indeed, the pore water [Na^+] at other sites such as ODP 1264 does not show a similar trend to Sites 807 and 806. We posit that reactions of the pore water with volcanic minerals at Sites 807 and 806 may have contributed to the high [Na^+] at depths. This is supported by the relatively high Na_2O content in the basalts at ODP 807C (Kroenke

et al., 1991). To simplify the model settings, although we do not think seawater [Na^+] has varied by more than a few percent, dynamic seawater [Na^+] records are used as the upper boundary condition, reflecting other potential Na sources to the pore water and thus higher [Na^+] in the pore water than in seawater.

APPENDIX C. SUPPLEMENTARY MATERIAL

Supplementary data to this article can be found online at https://doi.org/10.1016/j.gca.2021.04.012.

REFERENCES

Allen K. A., Hönisch B., Eggins S. M., Haynes L. L., Rosenthal Y. and Yu J. (2016) Trace element proxies for surface ocean conditions: a synthesis of culture calibrations with planktic foraminifera. *Geochim. Cosmochim. Acta* **193**, 197–221.

Allen K. A., Hönisch B., Eggins S. M. and Rosenthal Y. (2012) Environmental controls on B/Ca in calcite tests of the tropical planktic foraminifer species *Globigerinoides ruber* and *Globigerinoides sacculifer*. *Earth Planet. Sci. Lett.* **351–352**, 270–280.

Berner R. A. (1980) *Early diagenesis: a theoretical approach*. Princeton University Press, Princeton, NJ.

Berner R. A. and Kothavala Z. (2001) GEOCARB III: a revised model of atmospheric CO_2 over phanerozoic time. *Am. J. Sci.* **301**, 182–204.

Bertlich J., Nürnberg D., Hathorne E. C., De Nooijer L. J., Mezger E. M., Kienast M., Nordhausen S., Reichart G. J., Schönfeld J. and Bijma J. (2018) Salinity control on Na incorporation into calcite tests of the planktonic foraminifera *Trilobatus sacculifer* - Evidence from culture experiments and surface sediments. *Biogeosciences* **15**, 5991–6018.

Bonnin E. A., Zhu Z., Fehrenbacher J. S., Russell A. D., Hönisch B., Spero H. J. and Gagnon A. C. (2019) Submicron sodium banding in cultured planktic foraminifera shells. *Geochim. Cosmochim. Acta* **253**, 127–141.

Boyle E. A. and Keigwin L. D. (1985) Comparison of Atlantic and Pacific paleochemical records for the last 215,000 years: changes in deep ocean circulation and chemical inventories. *Earth Planet. Sci. Lett.* **76**, 135–150.

Branson O., Bonnin E. A., Perea D. E., Spero H. J., Zhu Z., Winters M., Hönisch B., Russell A. D., Fehrenbacher J. S. and Gagnon A. C. (2016) Nanometer-scale chemistry of a calcite biomineralization template: implications for skeletal composition and nucleation. *Proc. Natl. Acad. Sci.* **113**, 12934–12939.

Brennan S. T., Lowenstein T. K. and Cendon D. I. (2013) The major-ion composition of Cenozoic seawater: the past 36 million years from fluid inclusions in marine halite. *Am. J. Sci.* **313**, 713–775.

Broecker W. S. and Peng T.-H. (1982) *Tracers in the Sea*. Lamont-Doherty Geological Observatory, Palisades, NY.

Brown S. J. and Elderfield H. (1996) Variations in Mg/Ca and Sr/Ca ratios of planktonic foraminifera caused by postdepositional dissolution: evidence of shallow Mg-dependent dissolution. *Paleoceanography* **11**, 543–551.

Busenberg E. and Plummer L. N. (1985) Kinetic and thermodynamic factors controlling the distribution of SO_4^{2-} and Na^+ in calcites and selected aragonites. *Geochim. Cosmochim. Acta* **49**, 713–725.

Chou W. C., Sheu D. D., Lee B. S., Tseng C. M., Chen C. T. A., Wang S. L. and Wong G. T. F. (2007) Depth distributions of alkalinity, TCO2 and δ13CTCO2 at SEATS time-series site in the northern South China Sea. *Deep. Res. Part II* **54**, 1469–1485.

Delaney M. L., Bé A. W. H. and Boyle E. A. (1985) Li, Sr, Mg, and Na in foraminiferal calcite shells from laboratory culture, sediment traps, and sediment cores. *Geochim. Cosmochim. Acta* **49**, 1327–1341.

Dickson A. G. (1990) Thermodynamics of the dissociation of boric acid in potassium chloride solutions from 273.15 to 318.15 K. *J. Chem. Eng. Data* **35**, 253–257.

Dickson A. G. and Millero F. J. (1987) A comparison of the equilibrium constants for the dissociation of carbonic acid in seawater media. *Deep. Res.* **34**, 1733–1743.

Elderfield H. (1996) A biomineralization model for the incorporation of trace elements into foraminiferal calcium carbonate. *Earth Planet. Sci. Lett.* **142**, 409–423.

Evans D., Erez J., Oron S. and Müller W. (2015) Mg/Ca-temperature and seawater-test chemistry relationships in the shallow-dwelling large benthic foraminifera *Operculina ammonoides*. *Geochim. Cosmochim. Acta* **148**, 325–342.

Evans D. and Müller W. (2012) Deep time foraminifera Mg/Ca paleothermometry: nonlinear correction for secular change in seawater Mg/Ca. *Paleoceanography* **27**, PA4205.

Expedition 320/321 Scientists (2010) Site U1337. In Proc. IODP, 320/321 (eds. H. Pälike, M. Lyle, H. Nishi, I. Raffi, K. Gamage, A. Klaus, and the Expedition 320/321 Scientists). Integrated Ocean Drilling Program Management International, Inc., Tokyo.

Fantle M. S. (2010) Evaluating the Ca isotope proxy. *Am. J. Sci.* **310**, 194–230.

Fantle M. S. and DePaolo D. J. (2006) Sr isotopes and pore fluid chemistry in carbonate sediment of the Ontong Java Plateau: calcite recrystallization rates and evidence for a rapid rise in seawater Mg over the last 10 million years. *Geochim. Cosmochim. Acta* **70**, 3883–3904.

Füger A., Konrad F., Leis A., Dietzel M. and Mavromatis V. (2019) Effect of growth rate and pH on lithium incorporation in calcite. *Geochim. Cosmochim. Acta* **248**, 14–24.

Gabitov R. I. and Watson E. B. (2006) Partitioning of strontium between calcite and fluid. *Geochem. Geophys. Geosyst.* **7**, Q11004.

Griffith E. M., Paytan A., Caldeira K., Bullen T. D. and Thomas E. (2008a) A dynamic marine calcium cycle during the past 28 million years. *Science* **322**, 1671–1674.

Griffith E. M., Paytan A., Kozdon R., Eisenhauer A. and Ravelo A. C. (2008b) Influences on the fractionation of calcium isotopes in planktonic foraminifera. *Earth Planet. Sci. Lett.* **268**, 124–136.

Hasiuk F. J. and Lohmann K. C. (2010) Application of calcite Mg partitioning functions to the reconstruction of paleocean Mg/Ca. *Geochim. Cosmochim. Acta* **74**, 6751–6763.

Hauzer H., Evans D., Müller W., Rosenthal Y. and Erez J. (2018) Calibration of Na partitioning in the calcitic foraminifer *Operculina ammonoides* under variable Ca concentration: toward reconstructing past seawater composition. *Earth Planet. Sci. Lett.* **497**, 80–91.

Haynes L. L., Hönisch B., Dyez K. A., Holland K., Rosenthal Y., Fish C. R., Subhas A. V. and Rae J. W. B. (2017) Calibration of the B/Ca proxy in the planktic foraminifer *Orbulina universa* to Paleocene seawater conditions. *Paleoceanography* **32**, 580–599.

Haynes L. L., Hönisch B., Holland K., Rosenthal Y. and Eggins S. M. (2019) Evaluating the planktic foraminiferal B/Ca proxy for application to deep time paleoceanography. *Earth Planet. Sci. Lett.* **528** 115824.

Hess J., Bender M. L. and Schilling J. G. (1986) Evolution of the ratio of strontium-87 to strontium-86 in seawater from Cretaceous to present. *Science* **231**, 979–984.

Hess J., Stott L. D., Bender M. L., Kennett J. P. and Schilling J.-G. (1989) The Oligocene marine microfossil record: age assessments using strontium isotopes. *Paleoceanography* **4**, 655–679.

Heuser A., Eisenhauer A., Böhm F., Wallmann K., Gussone N., Pearson P. N., Nägler T. F. and Dullo W. C. (2005) Calcium isotope ($\delta^{44/40}$Ca) variations of Neogene planktonic foraminifera. *Paleoceanography* **20**, PA2013.

Honjo S. and Erez J. (1978) Dissolution rates of calcium carbonate in the deep ocean: an in situ experiment in the North Atlantic Ocean. *Earth Planet. Sci. Lett.* **40**, 287–300.

Horita J., Zimmermann H. and Holland H. D. (2002) Chemical evolution of seawater during the Phanerozoic. *Geochim. Cosmochim. Acta* **66**, 3733–3756.

Ishikawa M. and Ichikuni M. (1984) Uptake of sodium and potassium by calcite. *Chem. Geol.* **42**, 137–146.

Johnstone H. J. H., Lee W. and Schulz M. (2016) Effect of preservation state of planktonic foraminifera tests on the decrease in Mg/Ca due to reductive cleaning and on sample loss during cleaning. *Chem. Geol.* **420**, 23–36.

Kawabata T., Takeda Y., Hori M., Kandori K. and Yaji T. (2021) Partitioning of sodium into calcium carbonates synthesized at 10–40 °C : influence of organic ligands and temperature. *Chem. Geol.* **559** 119904.

Key R. M., Kozyr A., Sabine C. L., Lee K., Wanninkhof R., Bullister J. L., Feely R. A., Millero F. J., Mordy C. and Peng T. H. (2004) A global ocean carbon climatology: results from Global Data Analysis Project (GLODAP). *Global Biogeochem. Cycles* **18**, GB4031.

Kitano Y., Okumura M. and Idogaki M. (1975) Incorporation of sodium, chloride and sulfate with calcium carbonate. *Geochem. J.* **9**, 75–84.

Kozdon R., Kelly D. C., Kitajima K., Strickland A., Fournelle J. H. and Valley J. W. (2013) In situ δ^{18}O and Mg/Ca analyses of diagenetic and planktic foraminiferal calcite preserved in a deep-sea record of the Paleocene-Eocene thermal maximum. *Paleoceanography* **28**, 517–528.

Lear C. H., Elderfield H. and Wilson P. A. (2003) A Cenozoic seawater Sr/Ca record from benthic foraminiferal calcite and its application in determining global weathering fluxes. *Earth Planet. Sci. Lett.* **208**, 69–84.

Lee K., Kim T. W., Byrne R. H., Millero F. J., Feely R. A. and Liu Y. M. (2010) The universal ratio of boron to chlorinity for the North Pacific and North Atlantic oceans. *Geochim. Cosmochim. Acta* **74**, 1801–1811.

Li Y. H. and Gregory S. (1974) Diffusion of ions in sea-water and in deep-sea sediments. *Geochim. Cosmochim. Acta* **38**, 703–714.

Lowenstein T. K., Hardie L. A., Timofeeff M. N. and Demicco R. V. (2003) Secular variation in seawater chemistry and the origin of calcium chloride basinal brines. *Geology* **31**, 857–860.

Mezger E. M., de Nooijer L. J., Boer W., Brummer G. J. A. and Reichart G. J. (2016) Salinity controls on Na incorporation in Red Sea planktonic foraminifera. *Paleoceanography* **31**, 1562–1582.

Mezger E. M., de Nooijer L. J., Siccha M., Brummer G. J. A., Kucera M. and Reichart G. J. (2018) Taphonomic and ontogenetic Effects on Na/Ca and Mg/Ca in spinose planktonic foraminifera from the Red Sea. *Geochem. Geophys. Geosyst.* **19**, 4174–4194.

Mucci A. and Morse J. W. (1983) The incorporation of Mg^{2+} and Sr^{2+} into calcite overgrowths: influences of growth rate and solution composition. *Geochim. Cosmochim. Acta* **47**, 217–233.

Okumura M. and Kitano Y. (1986) Coprecipitation of alkali metal ions with calcium carbonate. *Geochim. Cosmochim. Acta* **50**, 49–58.

Olsen A., Key R. M., Van Heuven S., Lauvset S. K., Velo A., Lin X., Schirnick C., Kozyr A., Tanhua T., Hoppema M., Jutterström T., Steinfeldt R., Jeansson E., Ishii M., Pérez F. F. and Suzuki T. (2016) The global ocean data analysis project version 2 (GLODAPv2) - An internally consistent data product for the world ocean. *Earth Syst. Sci. Data* **8**, 297–323.

Parkman R. H., Charnock J. M., Livens F. R. and Vaughan D. J. (1998) A study of the interaction of strontium ions in aqueous solution with the surfaces of calcite and kaolinite. *Geochim. Cosmochim. Acta* **62**, 1481–1492.

Pearson P. N., Ditchfield P. W., Singano J., Harcourt-Brown K. G., Nicholas C. J., Olsson R. K., Shackleton N. J. and Hall M. A. (2001) Warm tropical sea surface temperatures in the Late Cretaceous and Eocene epochs. *Nature* **413**, 481–487.

Pelletier G., Lewis E. and Wallace D. (2007) CO2SYS.XLS: A calculator for the CO2 system in seawater for Microsoft Excel/VBA. Version 2.3. Wash. State Dept. of Ecology/Brookhaven Nat. Lab., Olympia, WA/Upton, NY.

Perez F. F. and Fraga F. (1987) A precise and rapid analytical procedure for alkalinity determination. *Mar. Chem.* **21**, 169–182.

Richter F. M. (1993) Fluid flow in deep-sea carbonates: estimates based on porewater Sr. *Earth Planet. Sci. Lett.* **119**, 133–141.

Richter F. M. and DePaolo D. J. (1988) Diagenesis and Sr isotopic evolution of seawater using data from DSDP 590B and 575. *Earth Planet. Sci. Lett.* **90**, 382–394.

Richter F. M. and DePaolo D. J. (1987) Numerical models for diagenesis and the Neogene Sr isotopic evolution of seawater from DSDP Site 590B. *Earth Planet. Sci. Lett.* **83**, 27–38.

Richter F. M. and Liang Y. (1993) The rate and consequences of Sr diagenesis in deep-sea carbonates. *Earth Planet. Sci. Lett.* **117**, 553–565.

Rosenthal Y., Boyle E. A. and Labeyrie L. (1997) Last glacial maximum paleochemistry and deepwater circulation in the Southern Ocean: evidence from foraminiferal cadmium. *Paleoceanography* **12**, 787–796.

Rosenthal Y., Field M. P. and Sherrell R. M. (1999) Precise determination of element/calcium ratios in calcareous samples using sector field inductively coupled plasma mass spectrometry. *Anal. Chem.* **71**, 3248–3253.

Rosenthal Y. and Lohmann G. P. (2002) Accurate estimation of sea surface temperatures using dissolution-corrected calibrations for Mg/Ca paleothermometry. *Paleoceanography* **17**, 1044.

Rosenthal Y., Lohmann G. P., Lohmann K. C. and Sherrell R. M. (2000) Incorporation and preservation of Mg in *Globigerinoides sacculifer*: implications for reconstructing the temperature and ^{18}O/^{16}O of seawater. *Paleoceanography* **15**, 135–145.

Russell A. D., Honisch B., Spero H. J. and Lea D. W. (2004) Effects of seawater carbonate ion concentration and temperature on shell U, Mg, and Sr in cultured planktonic foraminifera. *Geochim. Cosmochim. Acta* **68**, 4347–4361.

Sadekov A. Y., Eggins S. M., Klinkhammer G. P. and Rosenthal Y. (2010) Effects of seafloor and laboratory dissolution on the Mg/Ca composition of *Globigerinoides sacculifer* and *Orbulina universa* tests - a laser ablation ICPMS microanalysis perspective. *Earth Planet. Sci. Lett.* **292**, 312–324.

Sarmiento J. L. and Gruber N. (2006) *Ocean biogeochemical dynamics*. Princeton University Press, Princeton, NJ.

Segev E. and Erez J. (2006) Effect of Mg/Ca ratio in seawater on shell composition in shallow benthic foraminifera. *Geochem. Geophys. Geosyst.* **7**, Q02P09.

Shipboard Scientific Party (1991) Site 807. In Proc. ODP, Init. Repts., 130 (eds. L.W. Kroenke, W.H. Berger, T.R. Janecek, and the Shipboard Scientific Party). Ocean Drilling Program, College Station, TX. pp. 369–493.

Shipboard Scientific Party (1995) Site 926. InProc. ODP, Init. Repts., 154 (eds. W.B. Curry, N.J. Shackleton, C. Richter, and

the Shipboard Scientific Party). Ocean Drilling Program, College Station, TX. pp. 153–232.

Si W. and Rosenthal Y. (2019) Reduced continental weathering and marine calcification linked to late Neogene decline in atmospheric CO_2. *Nat. Geosci.* **12**, 833–838.

Tang J., Köhler S. J. and Dietzel M. (2008) Sr^{2+}/Ca^{2+} and $^{44}Ca/^{40}Ca$ fractionation during inorganic calcite formation: I. Sr incorporation. *Geochim. Cosmochim. Acta* **72**, 3718–3732.

Tesoriero A. J. and Pankow J. F. (1996) Solid solution partitioning of Sr^{2+}, Ba^{2+}, and Cd^{2+} to calcite. *Geochim. Cosmochim. Acta* **60**, 1053–1063.

Urey H. C. (1952) The Planets, Their Origins and Development. Yale University Press, New Haven, CT.

Watson E. B. (1996) Surface enrichment and trace-element uptake during crystal growth. *Geochim. Cosmochim. Acta* **60**, 5013–5020.

White A. F. (1978) Sodium coprecipitation in calcite and dolomite. *Chem. Geol.* **23**, 65–72.

Wilkens R. H., Westerhold T., Drury A. J., Lyle M., Gorgas T. and Tian J. (2017) Revisiting the Ceara Rise, equatorial Atlantic Ocean: isotope stratigraphy of ODP Leg 154 from 0 to 5 Ma. *Clim. Past* **13**, 779–793.

Wit J. C., De Nooijer L. J., Wolthers M. and Reichart G. J. (2013) A novel salinity proxy based on na incorporation into foraminiferal calcite. *Biogeosciences* **10**, 6375–6387.

Yoshimura T., Tamenori Y., Suzuki A., Kawahata H., Iwasaki N., Hasegawa H., Nguyen L. T., Kuroyanagi A., Yamazaki T., Kuroda J. and Ohkouchi N. (2017) Altervalent substitution of sodium for calcium in biogenic calcite and aragonite. *Geochim. Cosmochim. Acta* **202**, 21–38.

Zeebe R. E. and Tyrrell T. (2019) History of carbonate ion concentration over the last 100 million years II: revised calculations and new data. *Geochim. Cosmochim. Acta* **257**, 373–392.

Associate editor: Thomas M. Marchitto